

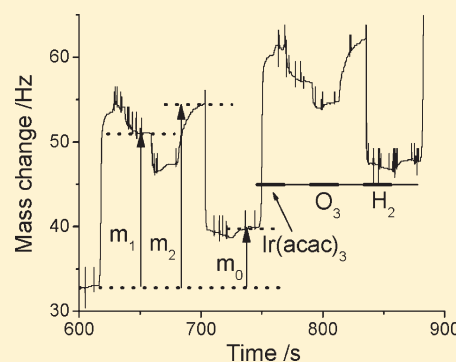
In situ Reaction Mechanism Studies on Atomic Layer Deposition of Ir and IrO₂ from Ir(acac)₃

Kjell Knapas* and Mikko Ritala

Laboratory of Inorganic Chemistry, Department of Chemistry, University of Helsinki, P.O. Box 55, FIN-00014 University of Helsinki, Finland

ABSTRACT: Reaction mechanisms in three atomic layer deposition (ALD) processes using Ir(acac)₃ as a precursor were studied: Ir(acac)₃–O₂ process at 300 °C for Ir deposition, Ir(acac)₃–O₃ process at 195 °C for IrO₂ deposition, and Ir(acac)₃–O₃–H₂ process at 195 °C for Ir deposition. Reactions were studied in situ with a quadrupole mass spectrometer (QMS) and a quartz crystal microbalance (QCM). The byproducts in all processes were CO₂ and H₂O. Only in the Ir(acac)₃–O₂ process these were partially released during the Ir(acac)₃ pulse (14% of CO₂ and 57% of H₂O as compared to a complete ALD cycle). To explain this, some oxygen atoms were concluded to chemisorb on the surface during the O₂ pulse. In the other two processes, the adsorption of Ir(acac)₃ appeared to be molecular on a plain surface of the film material.

KEYWORDS: iridium, iridium dioxide, atomic layer deposition, in situ, mass spectrometry, quartz crystal microbalance, reaction mechanism



INTRODUCTION

Iridium is one of the platinum metals (which phrase refers to elements 44–46 and 76–78), which all are noble, i.e. have positive standard electrode potentials. Because of this feature, iridium occurs preferably in metallic form and is as such very stable and highly resistant to oxidation, though many of its compounds are important too. The only well-established oxide of iridium is the conductive IrO₂, where the oxidation state of the metal is +IV, though iridium forms complexes as both +III and +IV.

Atomic layer deposition (ALD) is a superior method for thin film deposition.^{1–4} In ALD vapors of two or more precursors alternately react with the surface and saturate it with chemisorbed species. This self-limiting mechanism directly leads to successful deposition of uniform and conformal films with the desired composition and thickness, as soon as appropriate precursors are chosen, suitable reaction temperatures applied and correct numbers of deposition cycles performed. Numerous compounds have been deposited by ligand exchange reactions, reaction 1, in ALD fashion. In the equation, M^{m+} and A^{a–} are the cationic and anionic constituents of the film and Y[–] and R⁺ the Lewis bases and Lewis acids that carry the film constituents to the substrates. In some cases, entirely other kinds of reactions are applied, e.g., combustion mechanism when ozone is used as an oxygen source in many metal oxide deposition processes recently studied. However, ALD processes that deposit binary compounds generally always use separate precursors that supply the film constituents, and a great number of such processes can be developed indeed.



On the other hand, ALD of elements is not that straightforward. Some metals may be deposited by reducing metal precursors with, for example, H₂.⁴ For deposition of the platinum metals, however,

O₂ may be applied as the other precursor together with the metal complex.^{4,5} In these processes, molecular oxygen is activated through its dissociative chemisorption producing reactive atomic oxygen on the metal surface. Thermodynamically, these processes rely on the fact that no oxides of these metals are stable. They decompose spontaneously into the corresponding metals and O₂ at high enough temperatures. The platinum metal complex–O₂ ALD processes give the metals only at temperatures above certain threshold temperatures. It is thought that this threshold temperature is governed most likely by the dissociative chemisorption of O₂ on the metal surface. Below the threshold temperatures no reactions occur and nothing is deposited. The first such process to deposit iridium used Ir(acac)₃ (Hacac = acetylacetonone = 2,4-pentanedione) as an iridium source, and the threshold temperature of the Ir(acac)₃–O₂ process was 225 °C.⁶ Later, the same precursor was applied together with the more reactive oxidant, O₃, to deposit IrO₂ at temperatures below the threshold temperature of the Ir(acac)₃–O₂ process,⁷ about 200 °C. Above 210 °C, the Ir(acac)₃–O₃ process also deposited metallic iridium.⁷ Below 200 °C, metallic iridium was successfully deposited by executing a separate H₂ reduction step after each O₃ pulse, i.e., by applying a pulsing sequence of Ir(acac)₃–O₃–H₂.⁸ These references also include extensive and up to date disquisitions of application areas of iridium thin films in general⁶ and in integrated circuits, particularly⁵ ALD iridium processes⁸ and IrO₂ altogether, as well as various possible deposition methods for IrO₂.⁷

The surface reactions taking place during ALD processes are most competently clarified with in situ investigations. We use a quadrupole mass spectrometer (QMS) to study the composition of the gas phase and a quartz crystal microbalance (QCM) to

Received: December 7, 2010

Revised: April 20, 2011

Published: May 06, 2011

follow the mass development of the growing film.⁹ A further in situ method is infrared spectrometry (IR) that may be used to monitor both the gas phase and the surface species.^{10,11}

Among the platinum metal complex–O₂ ALD processes the mechanisms have been studied in situ so far for the ones using RuCp₂,¹² MeCpPtMe₃^{11–13} and Ir(acac)₃¹³ as precursors, and among O₃ based ALD processes for those using AlMe₃,^{10,14,15} InCp,¹⁶ (MeCp)₂Zr(OMe)Me,⁹ (Me₅Cp)Ti(OMe)₃¹⁷ and Hf(NEtMe)₄.^{15,18} Both combustion products and protonated ligands have been established as byproducts in all cases, except for the RuCp₂ and Ir(acac)₃ processes where only combustion products have been detected. In all the O₂ processes, and in the (MeCp)₂Zr(OMe)Me–O₃ and Hf(NEtMe)₄–O₃ processes, release of combustion products has been clearly observed not only during the O₂ or O₃ pulse but also during the metal precursor pulse. This may be either due to a combustion of the ligands during the metal precursor pulse by active oxygen left on the surface after the preceding O₃ or O₂ pulse, or due to a release of combustion product molecules previously formed but left adsorbed on the surface. Of the above-mentioned in situ techniques, only IR could distinguish between these two mechanisms, but even IR may have difficulties in distinguishing possible active oxygen species on oxide surfaces. Most often active oxygen, i.e. oxygen at oxidation state zero, has been concluded to be the case, however. In the paper at hand we present research on the mechanisms of all three previously mentioned Ir(acac)₃ processes, i.e., Ir(acac)₃–O₂ and Ir(acac)₃–O₃–H₂ for Ir, and Ir(acac)₃–O₃ for IrO₂ deposition, and compare these processes with each other and with processes studied in our above-mentioned earlier papers.

EXPERIMENTAL SECTION

The measurements were conducted in a specially modified¹⁹ ASM Microchemistry Ltd. F-120 SAT commercial hot-wall flow-type ALD reactor where films were deposited onto 3500 cm² of soda lime glass surface. The carrier gas was nitrogen (Oy Aga Ab, 99.999%). The QMS was a Hiden HAL/3F 501 RC using an ionization energy of 70 eV and a Faraday cup detector. The pressure was reduced from 3 mbar in the ALD reactor to 1×10^{-5} mbar in the QMS chamber by differential pumping through a 100 μ m orifice. The QCM was a Maxtek TM 400 applying a sampling rate of 20 Hz. The QCM was located downstream of the glass substrates, next to the QMS sampling orifice.

Ir(acac)₃ (ABCR GmbH & Co. KG, 99.9%) was held inside the reactor in an open boat at 165 °C and pulsed with inert gas valving.² For reference measurements In(acac)₃ was synthesized from InCl₃ and Hacac following literature methods²⁰ and held and pulsed similarly at 80 °C. Ozone (concentration 60 g/Nm³) was generated from oxygen (Oy Aga Ab, 99.999%) with a Wedeco Ozomatic Modular 4 HC Lab ozone generator. Ozone, oxygen (Oy Aga Ab, 99.9999%), hydrogen (Oy Aga Ab, 99.999%) and hydrogen sulfide (Messer Griesheim, 99.99%) were led into the reactor through needle and solenoid valves.

The studied processes were Ir(acac)₃–O₂ at 300 °C, Ir(acac)₃–O₃, and Ir(acac)₃–O₃–H₂ at 195 °C and for reference In(acac)₃–H₂S at 155 °C. Typically the pulse and purge times were 20 s. For the iridium processes, all trials saturating the substrates failed. Therefore, the glass substrates had to be removed from the reactor in order to start deposition at the QCM. In such a mode, the QCM begun to show growth in about 20 cycles. When the glass substrates were reinserted after such operation, deposition continued at the QCM, but it then took 15 s for Ir(acac)₃ to reach the QCM. We suspect these problems to be due to poor nucleation characteristics as typical for the noble metal ALD processes.

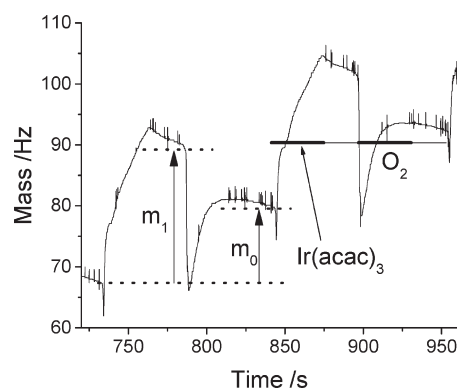


Figure 1. QCM results of the Ir(acac)₃–O₂ process.

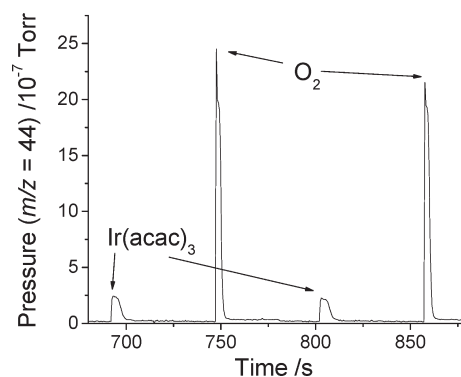


Figure 2. QMS results ($m/z = 44$, CO₂) of the Ir(acac)₃–O₂ process.

RESULTS AND DISCUSSION

Ir(acac)₃–O₂ Process. The Ir(acac)₃–O₂ process is known to deposit Ir at temperatures above 225 °C.⁶ QCM data for the process are shown in Figure 1. When the Ir(acac)₃ pulse reaches the crystal, the signal first descends fast a bit, but soon it starts ascending fast too; however, the ascent quickly slows down. During the O₂ pulse the signal first descends fast and then ascends slower to reach a plateau. The rapid descents in the beginning of both pulses may be caused by heating of the QCM by exothermic reactions.

As a result, the QCM measurements give $m_1/m_0 = 1.5 \pm 0.4$ ($N = 6$), where m_1 is the mass change during the Ir(acac)₃ pulse and the following purge, and m_0 the mass change during a complete ALD cycle. Whether the glass substrates are in the reactor or not does not affect this ratio. N is the number of measurements, and these have generally been done on different days after reloading the reactor. Therefore, they are to be considered genuine parallel measurements. The error limit is the standard deviation. Our result is the same as what was obtained previously,¹³ though in the previous paper the ratio was reported in the inverse way.

The only byproducts detected with QMS in the Ir(acac)₃–O₂ process were CO₂ and H₂O, the molecular peaks of which were seen in substantial amounts (Figures 2 and 3). Neither one of these topical m/z values showed any background signals for either precursor. $(14 \pm 2) \%$ ($N = 7$) of CO₂ and $(57 \pm 2) \%$ ($N = 7$) of H₂O were released already during the Ir(acac)₃ pulse as compared to a complete ALD cycle. During each reaction, the CO₂ release was completed much faster than the H₂O release.

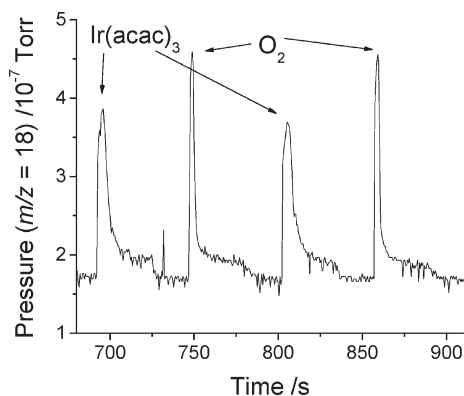
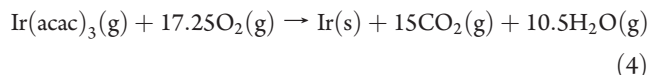
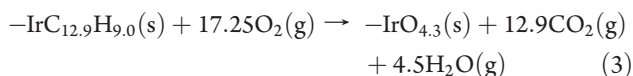
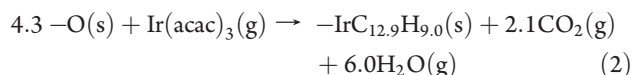


Figure 3. QMS results ($m/z = 18$, H_2O) of the $\text{Ir}(\text{acac})_3\text{--O}_2$ process.

No Hacac or any other possible reaction byproducts were detected. In the previous study,¹³ a somewhat smaller fraction, 4%, vs our 14%, of CO_2 was released during the $\text{Ir}(\text{acac})_3$ pulse. On the other hand, H_2O was not quantified in the previous study.

Assuming that CO_2 and H_2O are the only byproducts, our QMS results point to the half-reactions 2 and 3 constituting the overall reaction 4, which is complete combustion of the ligands. It is worth emphasizing that those equations indicate only in average what is being deposited on the surface. Therefore intermediates like $-\text{IrO}_{4.3}$ do not necessarily mean that all the oxygen atoms would be bonded to the single iridium atom deposited in reaction 2, but some of them are likely to be bonded to other iridium surface atoms that were there already before. The O_2 pulse leaves some adsorbed oxygen atoms on the surface, like was concluded with the $\text{RuCp}_2\text{--O}_2$ process.¹² The $\text{Ir}(\text{acac})_3$ molecules react with these oxygen atoms, whereby the ligands are partially combusted. Then the O_2 molecules complete the combustion of the ligands and reform the oxygen layer on the surface. Of course, there may also be some fixed amount of additional oxygen present all the time on the surface.



The above mechanism, deduced from the QMS results, gives $m_1 = M(\text{Ir}(\text{acac})_3) - 2.1M(\text{CO}_2) - 6.0M(\text{H}_2\text{O}) = 489.518 - 2.1 \cdot 44.01 - 6.0 \cdot 18.016 = 289$. Together with $m_0 = M(\text{Ir}) = 192.2$ this gives $m_1/m_0 = 1.50$, which is precisely the value obtained with QCM. Therefore, the QMS and QCM results and the suggested mechanism agree excellently. In the mechanism adsorbed oxygen atoms are assumed as reactive surface species as was earlier assumed with the $\text{RuCp}_2\text{--O}_2$ process.¹² Common to these processes are also the different fractions of carbon and hydrogen atoms combusted during the metal precursor pulse. In both cases, hydrogen is combusted in a substantially higher relative amount (57 and 90%) than carbon (14 and 50%). The exact nature of the surface species after the metal precursor pulse cannot be determined from the data at hand. IR might be able to provide information of these species.

On the other hand, the surface oxygen species after the oxygen pulse may be discussed now and compared with the ruthenium process. Assuming that all the adsorbed oxygen atoms participate in reaction 2, and knowing that the growth rate in the $\text{Ir}(\text{acac})_3\text{--O}_2$ process at 300°C is 0.46 \AA/cycle ,⁶ we can calculate the oxygen coverage after the O_2 pulse (reaction 3) and compare that with the saturation coverage of dissociatively chemisorbed O_2 on iridium that is known to be 1 ML at this temperature.²¹ The density of iridium is 22.4 kg/dm^3 , which translates to an atomic density of $7.018 \times 10^{28}\text{ atoms/m}^3$. From this the thickness of a monolayer (ML) $[(7.018 \times 10^{28})^{-1}\text{ m}^3]^{1/3} = 2.42 \times 10^{-10}\text{ m} = 2.42\text{ \AA}$. Therefore, the growth rate in the $\text{Ir}(\text{acac})_3\text{--O}_3$ process is $1/5.3\text{ ML/cycle}$. As 4.3 oxygen atoms are adsorbed per one iridium atom deposited (reaction 3), this corresponds to $4.3/5.3\text{ ML}$ which is about 80% of the saturation coverage of dissociatively chemisorbed O_2 . Accordingly, the $\text{Ir}(\text{acac})_3\text{--O}_2$ process does not need to involve any subsurface oxygen, whereas in the $\text{RuCp}_2\text{--O}_2$ process, subsurface oxygen was necessary to explain the results.¹²

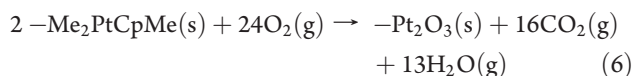
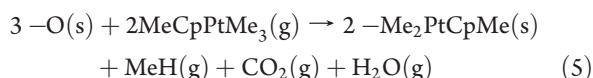
In the previous paper, on the other hand, hydroxyl groups were speculated as reactive surface species in the $\text{Ir}(\text{acac})_3\text{--O}_2$ process, and in the $\text{MeCpPtMe}_3\text{--O}_2$ processes.¹³ If this would be the case, Hacac would be expected to form as a byproduct during the $\text{Ir}(\text{acac})_3$ pulse. In fact, even in absence of surface hydroxyl groups, Hacac could still form as a byproduct, because water is anyway released during both pulses and may react further and give rise to protonated ligands. Generally, this would mean that water formed in combustion of ligands during the $\text{Ir}(\text{acac})_3$ pulse would release other ligands in protonated form still during the $\text{Ir}(\text{acac})_3$ pulse as was seen with the $(\text{MeCp})_2\text{Zr}(\text{OMe})\text{Me--O}_3$ process.⁹ Theoretically, Hacac could be released even during the O_2 pulse in the same way, but this would require the ligands to be more reactive toward water than O_2 , which obviously is not the case, since the $\text{Ir}(\text{acac})_3\text{--H}_2\text{O}$ process does not deposit anything. Anyhow, Hacac was not detected at any stage of the process either in this study nor in the previous one,¹³ even if it claimed formation of Hacac based on a complicated combustion quantification experiment.

To test if Hacac could have been released but still remained undetected, several tests were done. First Hacac was inserted directly into the reactor. In this experiment, QMS showed about equally strong signals at $m/z = 100$ (M^+) and $m/z = 85$ ($\text{M}^+ - \text{Me}$) and even a bit stronger signal at $m/z = 43$ (CH_3CO^+). Next, the $\text{In}(\text{acac})_3\text{--H}_2\text{S}$ process,²² where Hacac should be the byproduct, was run for reference and the mentioned m/z values measured. They could all be detected, though they were surprisingly weak. Extraordinary measures (recalibrating the m/z scale and adjusting the cage voltage) had to be taken to show them. Finally the $\text{Ir}(\text{acac})_3\text{--O}_2$ process was run again and the above m/z values measured with the optimized parameters. None of them could be detected, though it has to be pointed out that the sensitivity at $m/z = 43$ is here further weakened by the tail of $m/z = 44$. Furthermore, a couple of extra tests were performed. As results no Hacac was detected when pulsing $\text{Ir}(\text{acac})_3$ on an $-\text{OD}$ terminated Al_2O_3 surface or D_2O on an $-\text{acac}'$ terminated Ir surface. These observations together with the previous ones, and also the fact that the general success with β -diketonate–water ALD processes is almost nonexistent, suggest that no Hacac is formed in the $\text{Ir}(\text{acac})_3\text{--O}_2$ process, but that cannot be totally ruled out.

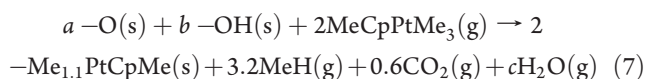
The possible role of hydroxyl groups may also be assessed based on their stabilities at the process temperatures. In ultrahigh vacuum and on single crystal specimens, with or without coadsorbed oxygen, all adsorbed water (also the water that has formed hydroxyl groups) desorbs from Ru, Rh, Pd, Ir and Pt

surfaces already below $-40\text{ }^{\circ}\text{C}$.²³ But then again, at higher pressures the saturation coverages of oxygen on the surfaces are larger, and the formation of hydroxyl groups accordingly more feasible. Therefore, on silica supported metals, hydroxyl groups are able to withstand evacuation up to $400\text{ }^{\circ}\text{C}$ on Pt and $200\text{ }^{\circ}\text{C}$ on Ir surfaces.²⁴ On the basis of this data, it would seem that hydroxyl groups could play a role in the $\text{MeCpPtMe}_3\text{--O}_2$ ALD process but not in the $\text{Ir}(\text{acac})_3\text{--O}_2$ process.

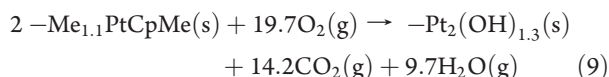
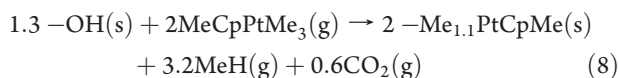
Next, let us briefly discuss literature results on the $\text{MeCpPtMe}_3\text{--O}_2$ process that is the most studied one of the platinum metal complex– O_2 processes.^{11–13} On the basis of the experimental observations, two alternatives, adsorbed oxygen and hydroxyl groups, have been suggested for the surface species with which the adsorbing MeCpPtMe_3 reacts. The only paper that states reaction equations,¹¹ concludes the mechanism of the process involving only adsorbed oxygen as reactive surface species and being



This was obtained with gas-phase IR without quantifying water. Water molecules forming in reaction 5 are partly released as such but partly protonate methyl ligands and release them as methane. The remaining ligands are combusted during the O_2 pulse (reaction 6). In the most recent paper,¹³ on the other hand, hydroxyl groups were considered as the reactive surface species. QMS and QCM agreed excellently, and it was found, also without quantifying water, that during the MeCpPtMe_3 pulse, for each reacting MeCpPtMe_3 molecule, 1.6 methyl ligands are released as methane and 0.3 methyl ligands combusted. Again, the O_2 pulse combusted completely the remaining ligands. With unknown amounts of surface oxygen atoms and hydroxyl groups and released water molecules, the observations during the MeCpPtMe_3 pulse in the most recent study lead to a reaction



Oxygen and hydrogen balances for this equation give that $a = c = 0$. Therefore, if the complicated quantification of the QMS and QCM results was successful and correct, the reactive surface species in the process should be hydroxyl groups and hydroxyl groups only. The half-reactions would then be



The third study on this process¹² used QMS only and clearly detected liberation of H_2O during the MeCpPtMe_3 pulse, and therefore would better support the first mechanism (reactions 5 and 6), though no quantification was done. Obviously, the mechanism of this process is not unambiguous but can vary depending on the experimental conditions, like different O_2 partial pressures and reactions on colder walls in reactors that do not exploit hot-wall configuration.

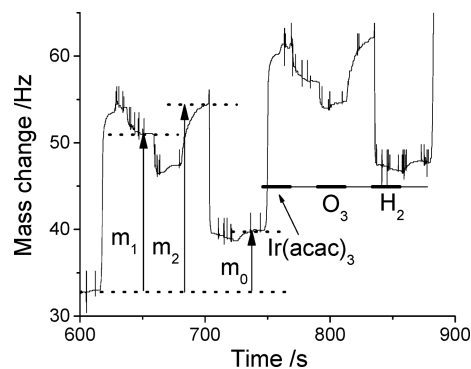


Figure 4. QCM results of the $\text{Ir}(\text{acac})_3\text{--O}_3\text{--H}_2$ process.

To summarize this part, we are convinced that our suggestion for the mechanism of the $\text{Ir}(\text{acac})_3\text{--O}_2$ process, reactions 2 and 3, is well-justified. Adsorbed oxygen atoms appear to be the reactive surface species for the adsorbing $\text{Ir}(\text{acac})_3$. In this respect, the process is similar to the $\text{RuCp}_2\text{--O}_2$ process,¹² but different from that process, no subsurface oxygen is needed and the chemisorbed amount suffices in the $\text{Ir}(\text{acac})_3\text{--O}_2$ process. The $\text{MeCpPtMe}_3\text{--O}_2$ process may differ from these in the respect that the reactive surface species can also be hydroxyl groups. This is due to the fact that hydroxyl groups are more stable on a platinum surface than on iridium surface.

$\text{Ir}(\text{acac})_3\text{--O}_3\text{--H}_2$ Process. The $\text{Ir}(\text{acac})_3\text{--O}_3\text{--H}_2$ process deposits Ir at lower temperatures ($165\text{--}200\text{ }^{\circ}\text{C}$) than the $\text{Ir}(\text{acac})_3\text{--O}_2$ process. At these temperatures exclusion of the H_2 pulses results in deposition of IrO_2 . QCM data for the $\text{Ir}(\text{acac})_3\text{--O}_3\text{--H}_2$ process are shown in Figure 4. During the $\text{Ir}(\text{acac})_3$ pulse, the signal ascends at first fast and then kind of settles, but during the following purge the signal descends a little. This is probably due to desorption of additional weakly adsorbed $\text{Ir}(\text{acac})_3$ molecules due to the lower temperature than in the previous process and because in this process $\text{Ir}(\text{acac})_3$ adsorbs molecularly (see below) rather than reactively (reaction 2). During the O_3 pulse, the signal descends to reach a plateau and during the following purge it ascends pretty much. The descent may here also be caused by heating of the QCM by exothermic reactions. Since no temporary descent is seen in the beginning of the $\text{Ir}(\text{acac})_3$ pulse, no exothermic reactions probably occur there, which is understandable since no oxygen should remain on the surface after the H_2 pulse. The absence of the mass descent in the beginning of the $\text{Ir}(\text{acac})_3$ pulse here and its presence in the process discussed above constitute additional evidence for the combustion reactions during the $\text{Ir}(\text{acac})_3$ pulse in the $\text{Ir}(\text{acac})_3\text{--O}_2$ process. Meanwhile, in the $\text{Ir}(\text{acac})_3\text{--O}_3\text{--H}_2$ process during the H_2 pulse the QCM signal descends fast indeed, directly obtains a plateau, and remains constant during the following purge.

The QCM measurements give $m_1/m_0 = 2.3 \pm 0.6$ ($N = 12$), where m_1 again is the mass change during the $\text{Ir}(\text{acac})_3$ pulse and purge and m_0 the mass change during a complete ALD cycle. Furthermore $m_2/m_0 = 2.6 \pm 0.5$ ($N = 12$), where m_2 is the mass change from the beginning of the $\text{Ir}(\text{acac})_3$ pulse to the end of the purge after the O_3 pulse. The meanings of the symbols m_0 , m_1 and m_2 are also displayed in Figure 4.

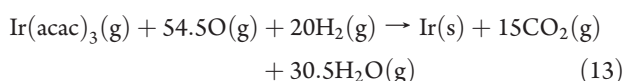
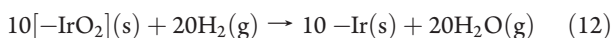
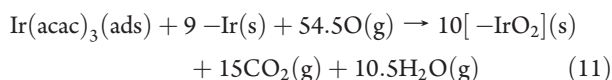
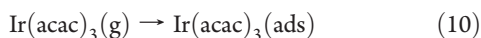
In this process, similar to the previous process, the only byproducts detected with the QMS were CO_2 and H_2O , of which the former is detected only during the O_3 pulse and the latter during the O_3 and the H_2 pulses. During the other pulses in the ALD process, the signals at $m/z = 44$ (CO_2^+) and $m/z = 18$

(H_2O^+) show straight lines at the base level. Importantly, no byproducts were detected during the $\text{Ir}(\text{acac})_3$ pulse, which is in clear contrast with the $\text{Ir}(\text{acac})_3\text{--O}_2$ process. Meanwhile, the signals show substantial backgrounds for all the precursors during which the corresponding byproduct is released. For CO_2 , this does not lead to a loss of information, because the unambiguous and only essential result is that it is released only during the O_3 pulse. However for H_2O it would be nice to calculate the ratio in which it is released during the O_3 and H_2 pulses. Unfortunately, the backgrounds during both pulses are so high, that the variation in this ratio is too great for such a determination to be worthwhile. Therefore, the mechanism will have to be determined here without quantification of water.

With this process also, no trace of Hacac as a byproduct was ever found. Accordingly, most likely it is not formed at all, though once again, that cannot be completely ruled out. Without Hacac or in general any byproducts released during the $\text{Ir}(\text{acac})_3$ pulse, the adsorption of $\text{Ir}(\text{acac})_3$ would have to take place molecularly on a plain iridium surface. This would give $m_1/m_0 = M(\text{Ir}(\text{acac})_3)/M(\text{Ir}) = 489.518/192.2 = 2.55$. The average experimental value is somewhat smaller, though 2.55 falls still within its error limits. Accordingly, the adsorption of $\text{Ir}(\text{acac})_3$ seems to be molecular indeed.

Next, since CO_2 is released only during the O_3 pulse, complete combustion of all the ligands evidently takes place during this pulse. Since furthermore no hydroxyl groups should remain on the surface (see above), the surface would have to incorporate only adsorbed oxygen atoms. From $m_2/m_0 = [M(\text{Ir}) + xM(\text{O})]/M(\text{Ir}) = [192.2 + 16x]/192.2 = 2.6$, we have $x = 20$. This means that for one adsorbed $\text{Ir}(\text{acac})_3$ molecule, i.e., for each iridium atom deposited, there will be 20 oxygen atoms deposited during the O_3 pulse. However, the reported growth rate of this process is only 0.22 \AA/cycle^8 which corresponds to $1/11 \text{ ML/cycle}$. Accordingly, the 20 oxygen atoms per adsorbed $\text{Ir}(\text{acac})_3$ molecule together with iridium atoms existing on the surface before the cycle correspond to a little less than one monolayer of IrO_2 . So, even here no real subsurface oxygen occurs, but there are about twice as many oxygen atoms on the surface than there were on an iridium surface saturated with the dissociatively chemisorbed O_2 . This is understandable, because IrO_2 itself is stable at the temperature applied, and because IrO_2 is deposited with the $\text{Ir}(\text{acac})_3\text{--O}_3$ process (see below).

During the H_2 pulse the oxygen atoms are removed as H_2O and the plain iridium surface restored. Accordingly, the mechanism of the $\text{Ir}(\text{acac})_3\text{--O}_3\text{--H}_2$ process appears to consist of (1) molecular adsorption of $\text{Ir}(\text{acac})_3$ on a plain iridium surface (reaction 10), (2) complete combustion of the ligands with O_3 giving also an oxidized surface (reaction 11), and (3) complete deoxidation restoring the plain iridium surface (reaction 12). The part-reactions sum up as the process reaction 13.



So, when we complicate the execution of the deposition with an extra step, we have a reaction mechanism much simpler than

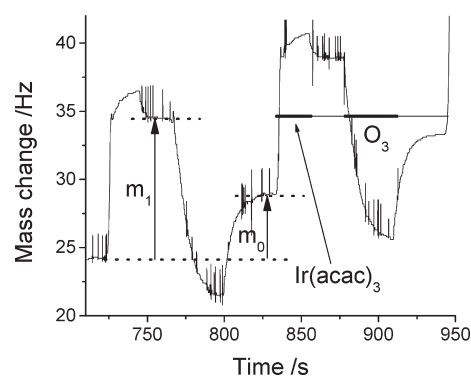
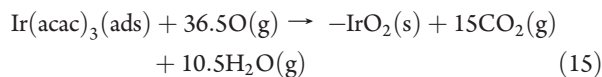
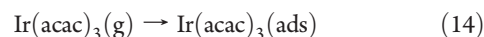


Figure 5. QCM results of the $\text{Ir}(\text{acac})_3\text{--O}_3$ process.

in many two-step processes. In this case, different from the $\text{Ir}(\text{acac})_3\text{--O}_2$ process, all the steps constitute reactions that advance as far as theoretically possible. This is mainly due to the high reactivities of ozone with hydrocarbons and hydrogen with oxygen. It should, however, also be noted that H_2 is generally found quite unreactive in ALD processes, and the feasibility of reaction 12 should be attributed specifically to oxygen in IrO_2 .

$\text{Ir}(\text{acac})_3\text{--O}_3$ Process. The $\text{Ir}(\text{acac})_3\text{--O}_3$ process deposits IrO_2 at temperatures below 200°C . QCM data for the process are shown in Figure 5. During the $\text{Ir}(\text{acac})_3$ pulse the signal looks about the same as in the $\text{Ir}(\text{acac})_3\text{--O}_3\text{--H}_2$ process. During the O_3 pulse however, the signal descends much more in the $\text{Ir}(\text{acac})_3\text{--O}_3$ process than in the $\text{Ir}(\text{acac})_3\text{--O}_3\text{--H}_2$ process, evidently because on the IrO_2 surface there are no metallic iridium atoms to react with ozone (cf. reaction 11). Common to the processes is then the about equal ascent during the purge after the O_3 pulse. The data in Figure 5 give $m_1/m_0 = 2.18$, which corresponds to molecular adsorption of $\text{Ir}(\text{acac})_3$. As in the two previous processes, the only byproducts found with QMS in this process were CO_2 and H_2O . They were released only during the O_3 pulses with straight lines at the base levels of the signals during the $\text{Ir}(\text{acac})_3$ pulses, thus clearly supporting the molecular adsorption of $\text{Ir}(\text{acac})_3$ in this ALD process (reaction 14). Interestingly, although oxygen atoms adsorbed on a metallic iridium surface in the $\text{Ir}(\text{acac})_3\text{--O}_2$ process above 225°C are oxidative toward the acac ligands (reaction 2), oxygen atoms in IrO_2 at 195°C are not. During the O_3 pulse, complete combustion of the ligands occurs and iridium is oxidized to IrO_2 (reaction 15). Essentially, these features are common with the $\text{Ir}(\text{acac})_3\text{--O}_3\text{--H}_2$ process.



When comparing this process to other O_3 ALD processes that deposit oxide films, one notices that this process is unique in that there are no reactive surface species for the metal precursor, but its adsorption is molecular. In some O_3 processes, especially those using AlMe_3 ,¹⁰ InCp ,¹⁶ and $(\text{Me}_3\text{Cp})\text{Ti}(\text{OMe})_3$ ¹⁷ as metal precursors, substantial amounts of hydroxyl groups have been recognized as reactive surface species. In those using $(\text{MeCp})_2\text{Zr}(\text{OMe})\text{Me}^9$ and $\text{Hf}(\text{NEtMe})_4$,¹⁵ a small amount of hydroxyl groups together with a relatively large amount of chemisorbed active oxygen have been found. This active oxygen seems to be somehow characteristic to the oxides of the heavier group 4 elements. At the same time, hydroxyl groups occur frequently on, for example, the

surfaces of Al_2O_3 and TiO_2 . With IrO_2 hydroxyl groups are unlikely as argued before, so the lack of reactive surface species is understandable here.

CONCLUSIONS

In the paper at hand, the reaction mechanisms of the $\text{Ir}(\text{acac})_3\text{--O}_2$ and $\text{Ir}(\text{acac})_3\text{--O}_3\text{--H}_2$ processes that deposit Ir and the $\text{Ir}(\text{acac})_3\text{--O}_3$ process that deposits IrO_2 were investigated. Only the first process was concluded to involve reaction of $\text{Ir}(\text{acac})_3$ upon its adsorption, as the adsorbed oxygen atoms combusted part of the ligands already during the $\text{Ir}(\text{acac})_3$ pulse. In the latter two processes, the adsorption of $\text{Ir}(\text{acac})_3$ was molecular on a plain surface of the film material.

AUTHOR INFORMATION

Corresponding Author

*E-mail: Kjell.Knapas@helsinki.fi.

ACKNOWLEDGMENT

Mr. Jani Hämäläinen is acknowledged for consultation and Ms. Miia Mäntymäki for synthesizing $\text{In}(\text{acac})_3$ for reference measurements.

REFERENCES

- (1) Suntola, T.; Antson, J. U.S. Patent 4 058 430, 1977.
- (2) Ritala, M.; Leskelä, M. In *Handbook of Thin Film Materials*; Nalwa, H. S., Ed.; Academic Press: San Diego, 2001, Vol. 1, Chapter 1.
- (3) Leskelä, M.; Ritala, M. *Angew. Chem., Int. Ed.* **2003**, *42*, 5548.
- (4) George, S. M. *Chem. Rev.* **2010**, *110*, 111.
- (5) Aaltonen, T. . *Ph.D. Thesis*, University of Helsinki, Helsinki, Finland, 2005; thesis available at <http://ethesis.helsinki.fi>.
- (6) Aaltonen, T.; Ritala, M.; Sammelselg, V.; Leskelä, M. *J. Electrochem. Soc.* **2004**, *151*, G489.
- (7) Hämäläinen, J.; Kemell, M.; Munnik, F.; Kreissig, U.; Ritala, M.; Leskelä, M. *Chem. Mater.* **2008**, *20*, 2903.
- (8) Hämäläinen, J.; Puukilainen, E.; Kemell, M.; Costelle, L.; Ritala, M.; Leskelä, M. *Chem. Mater.* **2009**, *21*, 4868.
- (9) Knapas, K.; Ritala, M. *Chem. Mater.* **2008**, *20*, 5698 and references therein.
- (10) Goldstein, D. N.; McCormick, J. A.; George, S. M. *J. Phys. Chem. C* **2008**, *112*, 19530.
- (11) Kessels, W. M. M.; Knoops, H. C. M.; Dielissen, S. A. F.; Mackus, A. J. M.; van de Sanden, M. C. M. *Appl. Phys. Lett.* **2009**, *95*, 013114.
- (12) Aaltonen, T.; Rahtu, A.; Ritala, M.; Leskelä, M. *Electrochem. Solid-State Lett.* **2003**, *6*, C130.
- (13) Cristensen, S. T.; Elam, J. W. *Chem. Mater.* **2010**, *22*, 2517.
- (14) Kwon, J.; Dai, M.; Halls, M. D.; Chabal, Y. J. *Chem. Mater.* **2008**, *20*, 3248.
- (15) Rose, M.; Niinistö, J.; Endler, I.; Bartha, J. W.; Kücher, P.; Ritala, M. *Appl. Mater. Interfaces* **2010**, *2*, 347.
- (16) Elam, J. W.; Martinson, A. B. F.; Pellin, M. J.; Hupp, J. T. *Chem. Mater.* **2006**, *18*, 3571.
- (17) Rose, M.; Niinistö, J.; Michalowski, P.; Gerlich, L.; Wilde, L.; Endler, I.; Bartha, J. W. *J. Phys. Chem. C* **2009**, *113*, 21825.
- (18) Wang, Y.; Dai, M.; Ho, M.-T.; Wielunski, L. S.; Chabal, Y. J. *Appl. Phys. Lett.* **2007**, *90*, 022906.
- (19) Rahtu, A.; Ritala, M. *Electrochem. Soc. Proc.* **2000**, *47*, 1354.
- (20) Kozacik, A. P.; Nygaard, E. M. U.S. Patent 2 654 769, 1953, example IV.
- (21) Taylor, J. L.; Ibbotson, D. E.; Weinberg, W. H. *Surf. Sci.* **1979**, *79*, 349.

(22) Yousfi, E. B.; Weinberger, B.; Donsanti, F.; Cowache, P.; Lincot, D. *Thin Solid Films* **2001**, *387*, 29.

(23) Shavorskiy, A.; Gladys, M. J.; Held, G. *Phys. Chem. Chem. Phys.* **2008**, *10*, 6150.

(24) Morrow, B. A.; Ramamurthy, P. *J. Phys. Chem.* **1973**, *77*, 3052.